PHYSICAL REVIEW B **80**, 161301(R) (2009)

# Response of nanocrystalline 3*C* silicon carbide to heavy-ion irradiation

W. Jiang,[1,*] H. Wang,[2] I. Kim,[2] I.-T. Bae,[3] G. Li,[1] P. Nachimuthu,[1] Z. Zhu,[1] Y. Zhang,[1] and W. J. Weber[1]
[1]*Pacific Northwest National Laboratory, P.O. Box 999, Richland, Washington 99352, USA*
[2]*Texas A&M University, College Station, Texas 77843, USA*
[3]*State University of New York at Binghamton, P.O. Box 6000, Binghamton, New York 13902, USA*
(Received 3 August 2009; published 9 October 2009)

Nanostructured materials are generally believed to be more radiation resistant. This study reports on Au-ion-induced amorphization in nanocrystalline 3*C*-SiC, characterized using x-ray diffraction, transmission electron microscopy and Raman spectroscopy. Full amorphization at room temperature occurs at a comparable dose to that for bulk SiC single crystals. The behavior is primarily attributed to a high ion flux and sluggish migration of point defects produced during irradiation. The results may have a significant implication of using nanophased SiC in extremely high radiation environments.

DOI: 10.1103/PhysRevB.80.161301 PACS number(s): 61.80.Jh, 61.43.Dq, 61.82.Rx

Silicon carbide (SiC) possesses excellent physical and chemical properties that make it a prominent candidate for a variety of applications. These include high-temperature, high-power and high-frequency microelectronic and opto-electronic devices, structural component in fusion reactors, cladding material for gas-cooled fission reactors, and an inert matrix for the transmutation of plutonium and other transuranics. Extensive experimental and theoretical research efforts have been devoted to the study of radiation effects in SiC single crystals over the past decades.[1–5] In general, bulk SiC crystals are readily amorphized under ion irradiation at room temperature.

It has been generally believed that nanostructured materials have a great potential to increase radiation resistance because of a large fraction of grain boundaries or interfaces that could absorb and annihilate mobile point defects produced during irradiation. With decreasing crystallite size, a shorter diffusion length is required for interstitials to reach the grain boundaries, where they could annihilate at unoccupied lattice sites to recover the defects. Similar processes could also take place for vacancy-type defects. As a result, defect accumulation in the interior of small crystalline particles could be minimized. To date, only a limited number of nanocrystalline materials have been investigated for radiation effects. Shen, *et al.*[6] found that magnesium gallium oxide ($MgGa_2O_4$) spinel in a nanocrystalline phase possesses a much higher radiation tolerance than in larger grained microstructures (average size of ~10 $\mu$m). In a separate study,[7] it has been demonstrated that damage accumulation in nanocrystalline TiN films is significantly less at a smaller crystallite size under $He^+$ ion irradiation. Previous studies also show that both nanocrystalline AlN (Ref. 8) and GaN (Ref. 9) are very resistant to amorphization under heavy-ion irradiation. However, in spite of the extremely high radiation hardness for amorphization in bulk form, nanostructured zirconia ($ZrO_2$) has been observed to be susceptible to amorphization due to excess surface free energy.[10] In contrast to extensive research results published on disordering and amorphization in SiC single crystals, reports on radiation effects in nanostructured SiC are still nonexistent, and disordering behavior of the material is currently unknown. It is an open question whether or under what conditions nanophased SiC behaves very differently from its bulk counterpart in the irradiation-induced disordering process. To address the scientific issues and gain a fundamental understanding, radiation effects in nanocrystalline SiC films have been recently studied, and the results are presented here.

Pulsed laser deposition (PLD) was used to grow polycrystalline SiC films on Si (001) at 973 K. The target was a hot-pressed stoichiometric SiC pellet with a purity of 99.95%. A KrF excimer laser ($\lambda=248$ nm) with a pulse rate of 5 Hz provided material ablation at an energy density of ~5 $J/cm^2$. Rutherford backscattering spectrometry (RBS) was followed to study the SiC films. The film thickness was determined to be ~360 nm based on the theoretical specific gravity of SiC (3.21 $g/cm^3$). A uniform concentration of C and Si was found over the entire thickness with a well-balanced composition of C and Si. No observable impurities of heavy elements were detected in the film. In addition, x-ray photoelectron spectroscopy (XPS) in combination with $Ar^+$ ion sputtering was also used to characterize the film prior to irradiation. The results indicate that there is a native surface oxidation layer of a few angstroms in thickness. The C to Si ratio in the interior of the film was determined to be about 1.0–0.9 without observable impurities, which is consistent with the RBS results.

Irradiation of the SiC film was performed using 2.0 MeV $Au^{2+}$ ions (normal incidence) at room temperature. The ion fluence was 6.9 $Au^{2+}/nm^2$, corresponding to a dose of ~0.5 dpa (displacements per atom) at the surface, ~3.0 dpa at the depth (~230 nm) of the damage peak, and ~1.2 dpa at the SiC/Si interface. A uniform beam intensity with a typical ion flux of $3.6\times10^{11}(Au^{2+}/cm^2)/s$ over an area of $12\times12$ $mm^2$ was achieved by using a beam rastering system.

Grazing incidence x-ray diffraction (GIXRD) at a fixed angle of $\omega=5°$ was used to study the irradiation effects in the SiC film. The diffractometer (Philips X'Pert MPD), operating at 45 kV and 40 mA, has a Cu $K\alpha$ source ($\lambda=1.541\,87$ Å) with a Göbel mirror for the incident beam and a 0.27 rad parallel-plate collimator for the diffracted beam. The results from the GIXRD measurements for the SiC film before and after irradiation are shown in Fig. 1. Predominant crystalline phase of the unirradiated film has been identified as polycrystalline cubic silicon carbide (3*C*-SiC) (PDF#: 04-008-7773) with the lattice parameter of $a=0.4439$ nm. Compared to bulk 3*C*-SiC single crystals (PDF#: 00-029-1129),

 ©2009 The American Physical Society

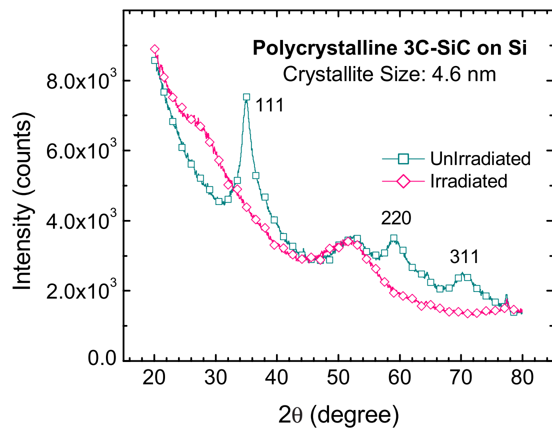


FIG. 1. (Color online) GIXRD patterns for a polycrystalline 3*C*-SiC film on Si (001) with an average crystallite size of 4.6 nm before and after irradiation with 2 MeV $Au^{2+}$ ions (normal incidence) to 6.9 ions/$nm^2$ at room temperature. The data suggest full amorphization following the irradiation.

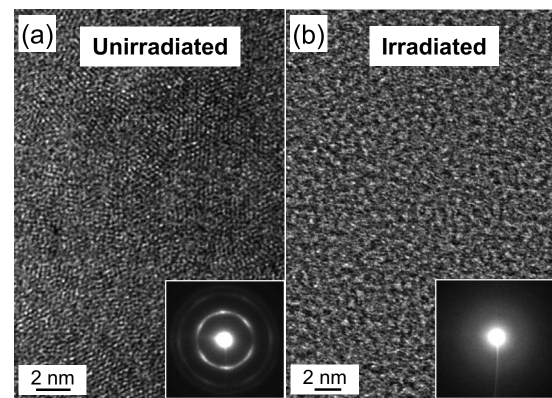


FIG. 2. HRTEM micrographs of the same sample as in Fig. 1 near the surface (a) before and (b) after irradiation. The insets show corresponding SAED patterns. The data suggest a crystalline to amorphous phase transformation in the SiC film.

the crystallites exhibit a relative lattice expansion of ~1.8%. The average crystallite size has been estimated to be 4.6 nm using the Scherrer formula based on the strongest diffraction peak of 3*C*-SiC (111). The small effects of lattice strain on the crystallite size are neglected in the estimation. As a result of the $Au^{2+}$ ion irradiation, distinct diffraction peaks of 3*C*-SiC (111), (220), and (311) disappear as shown in Fig. 1. The broad peak located at ~52° originates from a high-index in-plane reflection of the Si substrate. The results indicate that the polycrystalline 3*C*-SiC is fully amorphized under the irradiation conditions. In comparison, a continuously amorphized layer of ~670 nm in thickness, staring from the surface, was produced in 6*H*-SiC single crystal under the identical irradiation conditions (RBS/channeling data not shown).

To confirm full amorphization at the surface, where the dose is the lowest in the film, transmission electron microscopy (TEM) has been used to study the microstructures of the irradiated film. Cross-sectional thin foils of both unirradiated and irradiated samples were prepared using standard tripod wedge polishing, followed by ion thinning to electron transparency. The TEM microscope (JEOL JEM 2100F) was operated at 200 keV with a point-to-point resolution of 0.19 nm. Figure 2 shows the micrographs of the 3*C*-SiC films before and after irradiation. The high-resolution TEM (HRTEM) image in Fig. 2(a) clearly shows lattice fringes from the SiC crystalline grains before irradiation. The selected area electron-diffraction (SAED) pattern in the inset exhibits a Debye ring pattern associated with intensity maxima that are typical for polycrystalline materials with a preferred orientation. After irradiation, the lattice fringes in the HRTEM image disappear throughout the entire film thickness. The surface region of the irradiated SiC is shown in Fig. 2(b) with a SAED pattern in the inset that exhibits a halo pattern for the amorphized material. Since the minimum dose ( ~0.5 dpa) at the surface of the SiC film is comparable to the critical dose for amorphization with $Au^{2+}$ ion irradiation of single-crystal 6*H*-SiC (Ref. 11) and with $Ar^{2+}$ ion irradiation of single-crystal 3*C*-SiC (Ref. 12) at room temperature, there is no significant enhancement of radiation resistance of the polycrystalline SiC under the irradiation conditions.

Further studies have been performed using Raman backscattering with 514.5 nm excitation (Ar ion laser) at normal incidence. The laser beam was chopped by a mechanical shutter at a frequency of 1 Hz and had a power of 10–15 mW on the sample. No apparent damage to the sample surface was observed after the measurements. The results for the unirradiated and $Au^{2+}$-irradiated nanocrystalline and amorphous SiC under the same conditions (data acquisition time =400 s) are shown in Fig. 3. From Fig. 3(a), both Si-Si bonds at ~437 $cm^{-1}$ and C-C bonds at ~1445 $cm^{-1}$ are observed from amorphous grain boundaries in the unirradiated polycrystalline 3*C*-SiC. The peaks centered at ~810 and ~960 $cm^{-1}$ correspond to the transverse optical (TO) phonon mode[13] of 3*C*-SiC and a superposition of the longitudinal optical (LO) phonon mode[13] of 3*C*-SiC and second-order transverse-acoustic (2TA) phonon mode[14] of single-crystal Si, respectively. Small peak shifts might be due to the presence of lattice strain and defects in the nanocrystalline 3*C*-SiC. The strong, sharp peak (truncated in the figure) with the maximum counts of 56 170 at 520 $cm^{-1}$ is a remnant from the Si crystal substrate.[14] The overall background in the shift range may be contributed from the photoluminescence of the crystalline SiC. As a result of the $Au^{2+}$ irradiation, only three broad peaks are observed, corresponding to the contributions from the Si-Si, Si-C and C-C bonds of various atomic configurations in the amorphized material, as indicated in Fig. 3(a). This feature resembles that of ion-amorphized SiC single crystals, as reported previously.[15,16] The disappearance of both the sharp Si peak and the Si-2TA peak is due to amorphization of the SiC film that is less transparent to the visible light. These peaks are absent for even a thinner amorphous SiC film (310 nm thick) on Si (001) under the same Raman conditions, as shown in Fig. 3(b). Thus, the Si substrates, which are amorphized in the interface region as revealed by TEM in this study (data not shown), have negligible contributions to the Raman Si-Si peaks for the irradiated samples. From Figs. 3(a) and 3(b), the net areas of Si-C peaks decrease after irradiation, suggesting that Si-C bonds in the SiC films are dissociated during the ion irradiation. The larger areas of the Si-Si peaks for

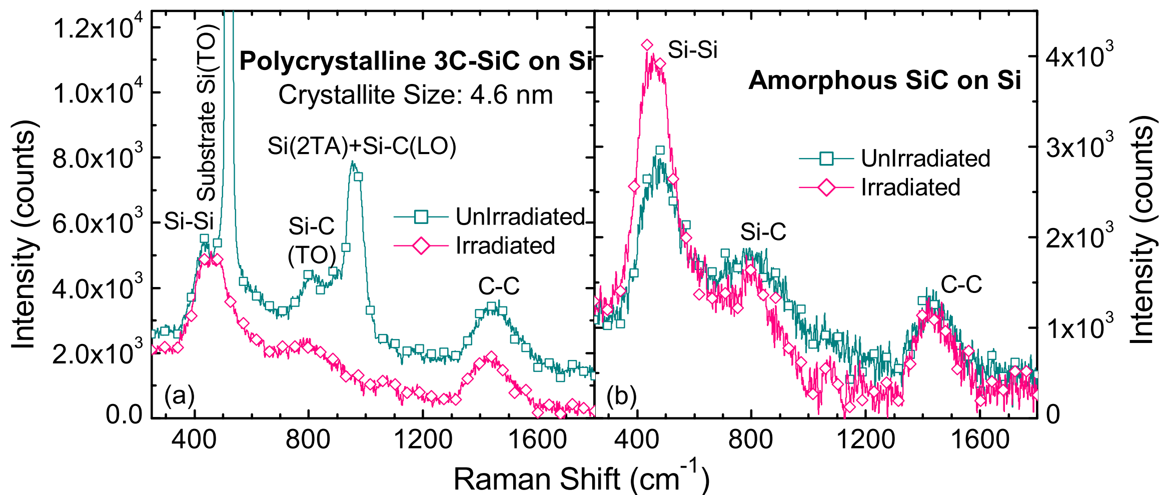


FIG. 3. (Color online) Raman spectra for (a) the same sample as in Fig. 1(b) an amorphous SiC film on Si (001) before and after irradiation. The data suggest dissociation of Si-C bonds and formation of homonuclear bonds during irradiation.

the irradiated samples are an indication of new Si-Si bond formation during the irradiation. The relative change in the C-C peak areas is small in Figs. 3(a) and 3(b), but formation of new C-C bonds is expected due to Si-C dissociation. Secondary ion mass spectroscopy (SIMS) for the two samples shows that Si or C diffusion does not occur at the interface nor in the film thickness before and after the irradiation, which is consistent with a previous study[16] of ion-amorphized 6*H*-SiC.

To understand the disordering behavior in nanocrystalline 3*C*-SiC, estimation of the diffusion kinetics is performed. In general, disorder accumulation in a crystalline grain cannot be avoided unless the point defects produced during irradiation are completely recovered before the next displacement event in the crystallite. The mean diffusion length, $l$, between the time, $t$, of two consecutive displacement events is given as $l=\sqrt{2Dt}$, where $D$ is the diffusion coefficient: $D=D_0\exp(-E_m/k_BT)$. $D_0$ is the pre-exponential factor, $E_m$ is the migration energy, $k_B$ is Boltzmann constant ($8.617\times10^{-5}$ eV/K), and $T$ is the absolute temperature. For simplicity, we consider a $4\times4\times4$ nm$^3$ cube of 3*C*-SiC crystallite with a face parallel to the sample surface. Since the ion flux in this study is $3.6\times10^{11}(\mathrm{Au}^{2+}/\mathrm{cm}^2)/\mathrm{s}$, the average time between two consecutive incoming $\mathrm{Au}^{2+}$ ions irradiating the cube is $t=17$ s/ion.

Experimentally, a slight temperature increase from 294 to 300 K during the MeV $\mathrm{Au}^{2+}$ ion irradiation was observed on the sample surface near the irradiation area. Since SiC has a high thermal conductivity, the temperature within the irradiation area is not expected to be much higher. We take 300 K in the following estimation of the defect kinetics. Hon *et al.*[17,18] measured the self-diffusion coefficients for $^{14}$C and $^{30}$Si in polycrystalline 3*C*-SiC with micron grain size in a temperature range from 2128–2547 K. The activation energy in their expressions is the sum of defect formation energy and defect migration energy. In ion-irradiated samples, point defects are created in the damage cascades, and diffusion of the defects depends only on defect migration energy. Because of the large discrepancy of the activation energy for C interstitial migration in 3*C*-SiC between experiment[17] and theory,[19] only Si diffusion kinetics is roughly calculated here. By substituting the activation energy in the expression[18] with Si migration energy (1.4 eV) via jumps of ⟨110⟩-oriented Si split interstitials,[19] the diffusion coefficients, $D$, at 300 K can be estimated to be $2.5\times10^{-16}$ cm$^2$/sec. Based on the value, the mean Si diffusion length, $l$, at room temperature is on the order of 0.93 nm. Similarly, according to molecular-dynamics (MD) simulations,[20] the mean diffusion length is estimated to be 1.2 nm and $4.7\times10^{-7}$ nm for C and Si interstitials in 3*C*-SiC, respectively. Since migration energies for C and Si vacancies are significantly higher,[19,20] their diffusion length is expected to be much smaller than 1 nm between the two consecutive displacement events at room temperature. Although the estimation is not expected to be accurate, the small values of $l$ for Si and C vacancies and interstitials, as compared to the distance (2 nm) required for point defects to reach the surface of the cube, suggest that disorder accumulation within the crystallites should occur under the experimental conditions. Consequently, disordering behavior in the nanocrystalline 3*C*-SiC should be similar to that in bulk 3*C*-SiC single crystals. Amorphization of the nanocrystalline material is likely a result of disruption of the crystalline structure through local defect accumulation and interaction. In addition to amorphization within the crystallites, contribution of amorphization at the grain boundary is also possible. Since a significant reduction in amorphization dose is not observed as compared to bulk SiC, interface-stimulated amorphization is not expected to be a dominant process under the experimental conditions.

Previous experimental studies[11] have shown room-temperature defect recovery in low-temperature Au-ion-irradiated SiC. Subsequent Monte Carlo simulations[21] have revealed that the recovery is primarily attributed to the recombination of close Frankel pairs in SiC. Although the point defects do not have enough time to diffuse to the grain boundary under the conditions of this study, possible "self recovery" might occur at a lower ion flux or a higher irradiation temperature based on the results of previous calculations[19] and simulations.[20] In addition, the presence of lattice strain and irradiation itself might enhance diffusion of

point defects in the crystal structure. Both ion flux and mobility of point defects, especially vacancies that migrate more slowly, are critical factors for the "self recovery" during irradiation. More studies are currently being performed and the results will be reported separately.

In conclusion, although many nanocrystalline materials exhibit an enhancement in radiation resistance, nanostructured polycrystalline 3*C*-SiC does not show a significantly different disordering behavior in this study as compared to its bulk material at room temperature. Like in SiC single crystals, lattice disorder accumulates in the 3*C*-SiC crystallites and amorphization occurs as a result of local defect accumulation and interaction. Both the high ion flux and sluggish migration of point defects at room temperature are responsible for the disordering behavior. At a lower ion flux or a higher irradiation temperature, disordering in SiC nanocrystals might behave differently, which requires further studies. During amorphization in the nanostructured 3*C*-SiC, dissociation of Si-C bonds and formation of homonuclear bonds are observed. The results from this study provide important information regarding lattice disordering in nanocrystalline SiC and may have significant implications for cautions of using the material in extremely high radiation environments at or below room temperature.

This research was supported by the Division of Materials Sciences and Engineering, Office of Basic Energy Sciences, U.S. DOE under Contract No. DE-AC05-76RL01830. A major part of the work was performed at EMSL, a DOE user facility located at PNNL. The work at Texas A&M University was supported by the National Science Foundation (Award No. 0846504). Support of $S^3$IP at SUNY Binghamton was provided by Empire State Development Corporation.

*Corresponding author; weilin.jiang@pnl.gov

[1] L. L. Snead, S. J. Zinkle, J. C. Hay, and M. C. Osborne, Nucl. Instrum. Methods Phys. Res. B **141**, 123 (1998).
[2] W. J. Weber, Nucl. Instrum. Methods Phys. Res. B **166-167**, 98 (2000).
[3] W. Jiang and W. J. Weber, Phys. Rev. B **64**, 125206 (2001).
[4] M. Ishimaru, I.-T. Bae, Y. Hirotsu, S. Matsumura, and K. E. Sickafus, Phys. Rev. Lett. **89**, 055502 (2002).
[5] Y. Zhang, F. Gao, W. Jiang, D. E. McCready, and W. J. Weber, Phys. Rev. B **70**, 125203 (2004).
[6] T. D. Shen, S. Feng, M. Tang, J. A. Valdez, Y. Wang, and K. E. Sickafus, Appl. Phys. Lett. **90**, 263115 (2007).
[7] H. Wang, R. Araujo, J. G. Swadener, Y. Q. Wang, X. Zhang, E. G. Fu, and T. Cagin, Nucl. Instrum. Methods Phys. Res. B **261**, 1162 (2007).
[8] W. Jiang, I.-T. Bae, and W. J. Weber, J. Phys.: Condens. Matter **19**, 356207 (2007).
[9] W. Jiang, W. J. Weber, L. M. Wang, and K. Sun, Nucl. Instrum. Methods Phys. Res. B **218**, 427 (2004).
[10] A. Meldrum, L. A. Boatner, and R. C. Ewing, Phys. Rev. Lett. **88**, 025503 (2001).
[11] W. Jiang, W. J. Weber, S. Thevuthasan, and V. Shutthanandan, J. Nucl. Mater. **289**, 96 (2001).
[12] W. J. Weber, N. Yu, and L. M. Wang, J. Nucl. Mater. **253**, 53 (1998).
[13] Z. C. Feng, A. J. Mascarenhas, W. J. Choyke, and J. A. Powell, J. Appl. Phys. **64**, 3176 (1988).
[14] J. Liu, J. Niu, D. Yang, M. Yan, and J. Sha, Physica E **23**, 221 (2004).
[15] W. Bolse, Nucl. Instrum. Methods Phys. Res. B **148**, 83 (1999).
[16] W. Jiang, Y. Zhang, M. H. Engelhard, W. J. Weber, G. J. Exarhos, J. Lian, and R. C. Ewing, J. Appl. Phys. **101**, 023524 (2007).
[17] M. H. Hon and R. F. Davis, J. Mater. Sci. **14**, 2411 (1979).
[18] M. H. Hon and R. F. Davis, J. Mater. Sci. **15**, 2073 (1980).
[19] M. Bockstedte, A. Mattausch, and O. Pankratov, Phys. Rev. B **68**, 205201 (2003).
[20] F. Gao, W. J. Weber, M. Posselt, and V. Belko, Phys. Rev. B **69**, 245205 (2004).
[21] Z. Rong, F. Gao, W. J. Weber, and G. Hobler, J. Appl. Phys. **102**, 103508 (2007).